of 0.6 and below. At higher $[MCPBA]_{t=0}$ and polymer concentration penetration of the crystal core of at least some parts of the lamellas can take place during epoxidation. It is concluded that essentially all of the noncrystalline material present can be reacted. Therefore the intramolecular defects are not appreciable and the density values can be used as a first approximation to calculate the average number of monomer units in a noncrystalline chain sequence, U, made up of folds and interlamellar links as done above.

Acknowledgment. This research was supported by grants from the National Science Foundation, Polymers Program (Grant No. DMR-8007226), and the Professional Staff Conference—Board of Higher Education of the City University of New York (Grant No. 13148).

Registry No. Polyisoprene (homopolymer), 9003-31-0.

References and Notes

(1) Schlesinger, W.; Leeper, H. M. *J. Polym. Sci.* **1953**, *11*, 203.
(2) Keller, A.; Martuscelli, E. *Makromol. Chem.* **1972**, *151*, 189.
(3) Flanagan, R. D.; Rijke, A. M. *J. Polym. Sci., Part A-2* **1972**, *10*, 1207.
(4) Anandakumaran, K.; Kuo, C. C.; Mukherji, S.; Woodward, A. E. *J. Polym. Sci., Polym. Phys. Ed.* **1982**, *20*, 1669.
(5) Anandakumaran, K.; Herman, W.; Woodward, A. E. *Macromolecules* **1983**, *16*, 563.
(6) Bunn, C. W. *Proc. R. Soc. London, Ser. A* **1942**, *180*, 40.
(7) Fisher, D. *Proc. Phys. Soc. London* **1953**, *66*, 7.
(8) Takahashi, Y.; Sato, T.; Tadokoro, H.; Tanaka, Y. *J. Polym. Sci., Polym. Phys. Ed.* **1973**, *11*, 233.
(9) Leeper, H. M.; Schlesinger, W. *J. Polym. Sci.* **1953**, *11*, 307.
(10) Geil, P. H. "Polymer Single Crystals"; Wiley: New York, 1963.
(11) Wunderlich, B. "Macromolecular Physics"; Academic Press: New York, 1973; Vol. 1.
(12) Andrews, E. H.; Owen, P. J.; Singh, A. *Proc. R. Soc. London, Ser. A* **1971**, *324*, 79.
(13) Davies, C. K. L.; Long, O. E. *J. Mater. Sci.* **1977**, *12*, 2165.
(14) Stellman, J. M.; Woodward, A. E. *J. Polym. Sci., Part B* **1969**, *7*, 755.
(15) Wichacheewa, P.; Woodward, A. E. *J. Polym. Sci., Polym. Phys. Ed.* **1978**, *16*, 1849.
(16) Tseng, S.; Herman, W.; Woodward, A. E.; Newman, B. A. *Macromolecules* **1982**, *15*, 338.
(17) Tseng, S.; Woodward, A. E. *Macromolecules* **1982**, *15*, 343.
(18) Cooper, W.; Vaughan, G. *Polymer* **1963**, *4*, 329.
(19) Fischer, E.; Henderson, J. F. *J. Polym. Sci., Part A-2* **1967**, *5*, 377.
(20) Woodward, A. E. *Polymer* **1964**, *5*, 293.
(21) Khoury, F.; Barnes, J. D. *J. Res. Natl. Bur. Stand., Sect. A* **1972**, *76*, 225.
(22) Khoury, F.; Barnes, J. D. *J. Res. Natl. Bur. Stand., Sect. A* **1974**, *78*, 95.
(23) Barnes, J. D.; Khoury, F. *J. Res. Natl. Bur. Stand. Sect. A* **1974**, *78*, 363.
(24) Maxfield, J.; Mandelkern, L. *Macromolecules* **1977**, *10*, 550.
(25) Allen, R. C.; Mandelkern, L. *J. Polym. Sci., Polym. Phys. Ed.* **1982**, *20*, 1465.
(26) Davies, C. K. L.; Long, O. E. *J. Mater. Sci.* **1979**, *14*, 2529.
(27) Hamada, F.; Wunderlich, B.; Sumida, T.; Hayashi, S.; Makajima, A. *J. Phys. Chem.* **1968**, *72*, 178.
(28) Banks, W.; Gordon, M.; Roe, R.-J.; Sharples, A. *Polymer* **1963**, *4*, 61.
(29) Maclaine, J. Q. G.; Booth, C. *Polymer* **1975**, *16*, 680.
(30) Se, K.; Adachi, K.; Kotaka, T. *Polym. J.* **1981**, *13*, 1009.
(31) Marco, C.; Fatou, J. G.; Bello, A. *Polymer* **1977**, *18*, 1100.
(32) Marco, C.; Fatou, J. G.; Bello, A.; Blanco, A. *Polymer* **1979**, *20*, 1250.
(33) Schilling, F. C.; Bovey, F. A.; Tseng, S.; Woodward, A. E. *Macromolecules* **1983**, *16*, 808.

Forces between Two Adsorbed Poly(ethylene oxide) Layers in a Good Aqueous Solvent in the Range 0–150 nm

Jacob Klein*† and Paul F. Luckham

Physics and Chemistry of Solids, Cavendish Laboratory, Cambridge, CB3 0HE U.K.
Received August 29, 1983

ABSTRACT: We have measured the forces $F(D)$ between two smooth curved mica surfaces a distance D apart immersed in 0.1 M KNO_3, both in the absence and in the presence of adsorbed layers of monodispersed poly(ethylene oxide), of two molar masses M (40 000 and 160 000). Interactions between the bare surfaces are characteristic of electrostatic double-layer overlap, and strongly repulsive for $D \lesssim 8$ nm. Following adsorption of the polymer, the main features of the interactions are as follows: (i) On a first approach of the surfaces following adsorption and on subsequent compression/decompression cycles that are sufficiently slow to allow relaxation of the polymer on the surfaces ($\gtrsim$1 h), a *quasi-equilibrium* $F(D)$ profile is indicated. The onset of repulsive interactions occurs at $D \simeq 6 \pm 1\ R_g$ (the respective radii of gyration for the two molar masses), and $F(D)$ is increasingly repulsive at lower D values. (ii) More rapid ($\sim$5 min) compression/decompression cycles reveal time-dependent effects. The general observation in these cases is that $F(D)$ is lower for any given D than the corresponding quasi-equilibrium value. (iii) The adsorbance of polymer is 4 ± 1.5 mg m^{-2}, and adsorption is irreversible over the times of our experiments. (iv) There is no evidence for attraction or adhesion between the surfaces once the equilibrium adsorption has been attained. Our results contrast with an earlier report for a similar system but utilizing a commercial-grade polymer (Israelachvili et al. *J. Colloid Interface Sci.*, 78, 432 (1980)), in particular as regards our observations of an equilibrium force–distance profile.

Introduction

The use of adsorbed macromolecules to stabilize colloidal dispersions (e.g., inks and paints) has a long history, and such steric stabilization has been intensively studied over the past few decades.[1] Most of these studies have involved the investigation of conditions under which polymer-coated colloidal dispersions retain (or lose) their stability, while only very few, relatively recently, have attempted to measure directly steric interaction forces between adsorbed macromolecular layers.[2-4]

Surface-balance[5] and compression-cell[6] techniques have been used to measure the pressure between colloidal particles in two- and three-dimensional arrays. More recently, van Vliet and Lyklema[2] measured the disjoining pressure between layers of polymers adsorbed at the two liquid–air interfaces of a film of polymer solution as a function of film thickness; Cain et al.[3] measured the force as a function of distance between layers of polymers adsorbed onto silicon rubber spheres, using the rubber de-

† Also Polymer Department, Weizmann Institute, Rehovot, Israel.

0024-9297/84/2217-1041$01.50/0

formation to measure the repulsion between the adsorbed layers. These methods are limited by the disadvantage of not being able to measure attraction, if any, between the adsorbed layers.

Israelachvili and co-workers,[4] modifying an approach pioneered by Tabor and co-workers,[7,8] measured the interaction $F(D)$ as a function of distance D between two smooth mica sheets immersed in an aqueous solution of a polydisperse commercial-grade resin of poly(ethylene oxide); the experimental technique they used is capable of measuring both attraction and repulsion. Their results showed strong hysteretic effects and in particular indicated a continuous buildup with time of adsorbed-layer thickness; for this reason they could not be described in terms of an equilibrium force–distance relationship.

Using a further modification of the mica apparatus, one of us[9] measured the interaction between adsorbed layers of monodispersed polystyrene in cyclohexane under poor solvent conditions ($T < \Theta$ temperature). In this case a *quasi-equilibrium force profile* $F(D)$ was observed: interaction between the polymer-bearing surfaces was initially *attractive* (at $D \sim 3R_g$, the unperturbed radius of gyration of the polystyrene used), becoming repulsive at $D \lesssim R_g$. The form of $F(D)$ was interpreted in terms of the osmotic interactions between the adsorbed segments at $T < \Theta$. These measurements were very recently extended by heating the polystyrene/cyclohexane system to $T \gtrsim \Theta$, where a force law showing some persistence of the attraction was obtained.[10]

We report here a study of the interactions between adsorbed poly(ethylene oxide) layers on mica surfaces, immersed in an aqueous electrolyte under *good solvent* conditions; the experimental approach is similar to that described earlier.[9] We have taken particular care to work with purified, monodispersed and well-characterized polymer (of two molecular masses) as for the earlier experiments in poor solvent conditions.[9] We have determined both the quasi-equilibrium force laws and also effects depending on the *rates* at which the adsorbed polymer layers were compressed and decompressed. A brief account of our main findings has appeared elsewhere.[11]

Experimental Section

The experimental approach is based on that developed by Tabor and co-workers[7,8] to measure forces between atomically smooth, curved mica surfaces in a crossed-cylinder configuration in air and vacuum; it was later extended by Israelachvili and co-workers to the case of liquid media[12] and by one of us to the case of polymer solutions.[9]

The present apparatus is similar to that described by Israelachvili and Adams;[12] the main difference is that for most of the present study the mica surfaces are enclosed by a small quartz cell, connected to the outside of the main stainless-steel box by teflon tubes. The volume of liquid required to immerse the mica surfaces is thus considerably smaller (~30 mL) than is the case when the whole of the box is filled (~350 mL), requiring smaller quantities of polymer for a given solution concentration; in addition, the cell is more convenient to clean, and its use greatly reduces the number of components coming in contact with the polymer solution. In one or two cases experiments were carried out filling the volume of the whole box with liquid; the results were identical with those obtained when the quartz cell was used.

The experimental technique has been described previously.[9,12] It is based on interferometry of white light undergoing multiple reflections between half-silvered, curved mica sheets. Observations of the resulting fringes of equal chromatic order (FECO) using a spectroscope (Glenn–Creston $^1/_2$ meter, dispersion 16 Å/mm) enables the determination of (i) the separation D between the mica surfaces, to ±0.3 nm in the range 0–200 nm, and the forces $F(D)$ between them (to ±50 nN), (ii) the mean refractive index of the medium separating the surfaces, and (iii) the geometry of the contact zone near the position of closest approach—in effect the mean radius of curvature R of the mica sheets in the cross-cylinder configuration.

Table I
Molecular Characteristics of the Poly(ethylene oxide) Samples

sample	M_W	M_W/M_N	R_g, nm
PEO1	1.60×10^5	1.04	13.0
PEO2	4.0×10^4	1.03	6.5

Prior to an experiment the glass, delrin, and stainless steel components which come in contact with the liquid, were exhaustively cleaned, as described previously.[9] The mica sheets were mounted, the apparatus was closed, and the air-contact FECO wavelengths were noted. Sufficient electrolyte solution (0.1 M KNO_3) was introduced into the cell to cover the mica surfaces, and $F(D)$ measured. The surfaces were withdrawn to $D \sim 3$ mm, and the polymer was introduced to the required concentration c (c = 10 and 150 μg mL^{-1} in these experiments). The surfaces were then left for 16 ± 2 h to incubate with the polymer solution, to allow adsorption to take place, following which $F(D)$ was measured. Finally, the polymer solution in the cell was diluted ~1000-fold by two successive replacements of the original solution by pure electrolyte, and $F(D)$ measured again. Cycles of decreasing and increasing D (compression and decompression) were carried out; the time for a cycle varied between ~10 min and ~1 h, and the intervals between cycles varied from ~1 min to several hours over a total period for an experiment of 1–3 days. Temperatures were monitored with a thermometer near the apparatus and were in the range 23 ± 2 °C throughout. All results reported are based on at least two independent experiments (different pairs of mica sheets or different contact positions).

Materials

Chemicals were B.D.H. analytical grade material and used as received. All water was freshly double distilled from a fused-silica–glass apparatus. Glassware was cleaned by immersion in sulphachromic acid for several hours and rinsed with water prior to use.

The poly(ethylene oxide) used was obtained from Toyo Soda Co. Ltd. (Japan) and was prepared via anionic polymerization of ethylene oxide. The molecular characteristics of the samples used, Table I, were determined by GPC (manufacturers data). Polymer solutions were made up to concentrations 10 ± 1 and 150 ± 5 μg mL^{-1}; both pure electrolyte and polymer solutions were filtered (Millipore 0.22 μm) prior to use.

The mica was best quality ruby muscovite (Kenya), grade 2 FS/GS, supplied by Mica and Micanite Ltd. (U.K.).

Results

Before introducing polymer into the system in any of the experiments, the force between the bare mica surfaces immersed in electrolyte was first measured. Figure 1 shows log $(F(D)/R)$ plotted against closest distance D between the mica surfaces, where R is their mean radius of curvature. In the Derjaguin approximation[13] (very nearly exact for $R \gg D$ as in the present case)

$$F(D)/R = 2\pi E(D) \quad (1)$$

where $E(D)$ is the interaction *energy* per unit area of flat *parallel* surfaces a distance D apart, obeying the same force law as the curved surfaces. The results correspond closely to electrostatic double-layer overlap repulsion expected from DLVO theory,[14,15] which predicts the exponential dependence corresponding to the straight line in Figure 1, and also to earlier accounts for the same system.[12] We have also noted, in accordance with the earlier work of Israelachvili and Adams,[12] a hysteretic behavior (open squares) on a first approach of the surfaces; on subsequent cycles the $F(D)$ profile moves closer in. The secondary

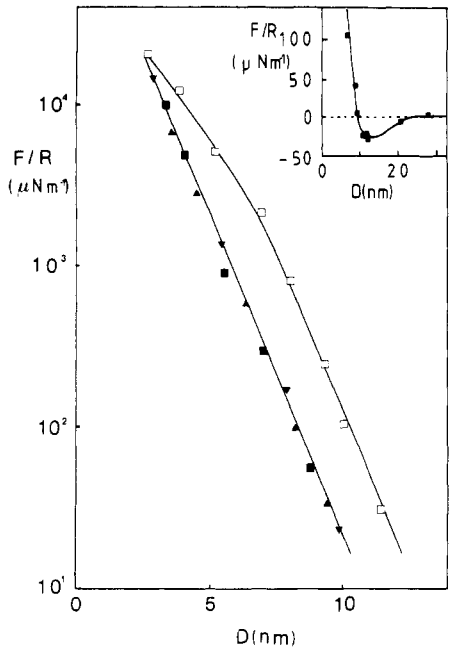

Figure 1. Force (F)–distance (D) profile between curved mica surfaces (mean radius R) in 0.1 M KNO_3 aqueous electrolyte (pH 5.5): (□) first compression of surfaces (decreasing D); (■) first decompression; (▼, ▲) second and subsequent compression/decompression cycles. Inset shows a profile around $F(D) \simeq 0$ on a linear–linear scale.

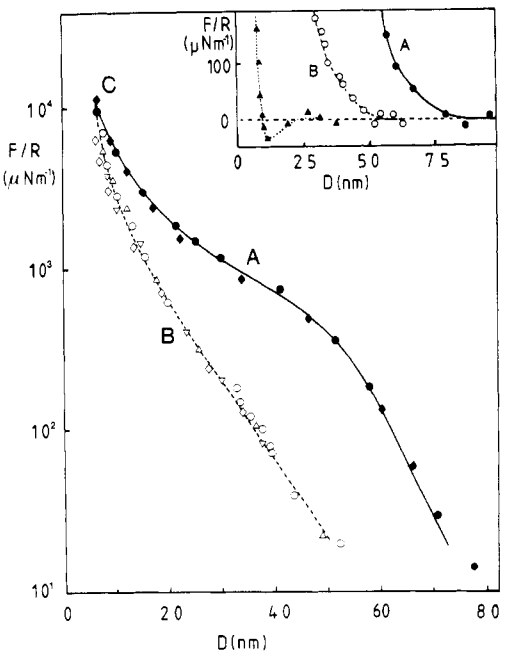

Figure 2. Force–distance profile between curved mica surfaces in 10 μg mL^{-1} PEO1 solution in 0.1 M KNO_3, following 16 ± 2 h incubation in the solution: (●) first compression of surfaces following incubation; (○) rapid decompression following '●'; (△) immediate rapid recompression following '○'; (▽) rapid decompression following '△'; (♦) compression 1 h after a decompression to large D (≳300 nm); (◇) rapid decompression following '♦'. Inset shows (F/R) vs. D on a linear–linear scale: (▲) interactions in 0.1 M KNO_3 prior to addition of polymer (from Figure 1); (●, ○) as for main diagram.

minimum in the force–distance profile (inset) is due to the strong screening of the double-layer repulsion forces at the high salt concentration used (0.1 M KNO_3, Debye length $\simeq$ 1.1 nm), and the consequent dominance of Van der Waals attraction at $D \gtrsim 10$ nm.

Figure 2 shows the force profiles determined after introducing PEO1 (M = 160 000) into the electrolyte to a concentration c = 10 μg mL^{-1} and allowing the surfaces to incubate at $D \sim 3$ mm for 16 h; the results are presented as a log–linear plot to enable presentation of several orders of magnitude variation in $F(D)$. The main features of the profiles in Figure 2 are characteristic of this system and were observed in varying degree at other values of the incubating concentration c and polymer molecular mass M. For this reason we shall describe them in some detail, in particular the effect on $F(D)$ of compression/decompression rates.

On a first approach following incubation, no interaction was measurable from large D down to $D \sim 75$ nm (see also inset to Figure 2, showing F vs. D on a linear–linear scale), when a monotonically increasing repulsion was observed (curve A of Figure 2) down to $D \sim 6$ nm (point C on Figure 2).

Subsequent behavior on *decompression* (i.e., increasing surface separation D) depended on the rate at which it was carried out. For a rapid decompression (i.e., 5–8 min for D going 6–60 nm: this period was determined by the minimum time required to make the actual measurements) $F(D)$ followed the broken curve B, becoming indistinguishable from zero at $D \gtrsim 50$ nm (on decompression, the surfaces were generally taken out to $D \sim 200$ nm). If the surfaces were again recompressed *immediately following* the rapid decompression (within ~1 min), the resulting force–distance profile again followed the broken curve B. On the other hand, if a long period (~1 h) was allowed to elapse between a rapid decompression and the next compression, the force–distance profile followed (within error) *curve A* rather than curve B. For a *slow decompression* from the point C (i.e., ≳1 h for D going 6–80 nm), the force profile followed curve A again.

The general, and reproducible, features may be summarized as follows: (i) Compression of the surfaces after they had been apart for an hour or more led to curve A on the F vs. D profile (Figure 2). (ii) Slow decompression, and subsequent compression, also followed curve A. (iii) Rapid decompression, and also immediate subsequent compression, followed curve B.

For intermediate cases (e.g., waiting for say ~10 min following a rapid decompression) the F/R vs. D plot fell in the region between A and B. To investigate this more systematically, a slow decompression was carried out as in Figure 3 (for the same polymer and conditions as in Figure 2). The surfaces were withdrawn from the point A_n (where A_1 in Figure 3 corresponds to the point C in Figure 2) to the point B_n, where the force was measured; the system was left for 15 min, while the surfaces moved out spontaneously to A_{n+1}, where $F(D)$ was again determined, and then once again the surfaces were withdrawn to B_{n+1}, and so on. Figure 3 shows how the points A_n quite closely follow curve A in Figure 2, while the points B_n fall in the region between curves A and B in Figure 2. (It should be noted that due to the length of time involved in this slow separation experiment, cumulative absolute errors, due to random thermal drift of the surfaces, of up to ~100 μN m^{-1} may be present by the end of the decompression. The *relative* error between any two points B_n and A_{n+1} will be considerably smaller.)

The force–distance profile following incubation in 150 μg mL^{-1} solution of PEO1 (as opposed to 10 μg mL^{-1} as in Figures 2 and 3) is shown in Figure 4. The characteristic "relaxed" and "unrelaxed" profiles, corresponding to A and B in Figure 2, are clearly seen; the magnitude of $F(D)$ in Figure 4, however, is about twice its value in Figure 2, for any given D. Also shown in Figure 4 are data obtained following replacement of the polymer solution by

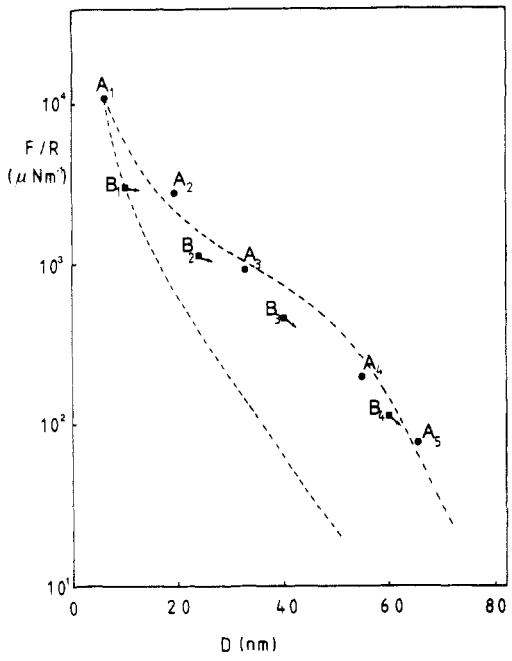

Figure 3. Force–distance profile for same conditions as Figure 2, for slow decompression. Surfaces taken from A_n to B_n, and then left for 15 min, whereon they relax spontaneously (→) to the position A_{n+1}, and so on. Further details in text.

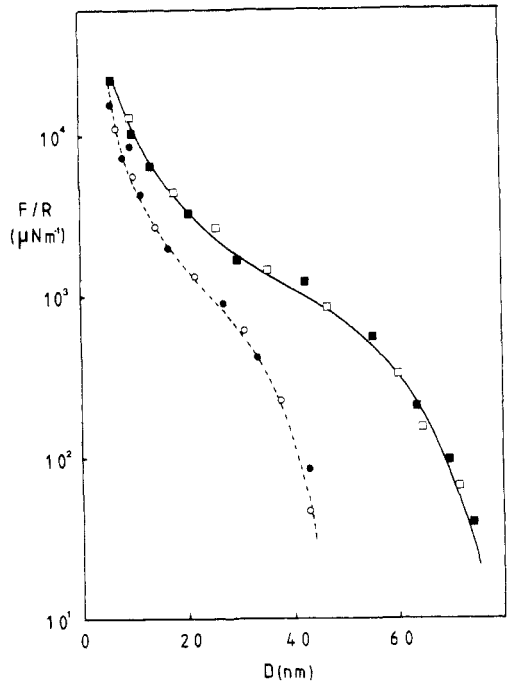

Figure 4. Force–distance profile between mica surfaces following 16 ± 2 h incubation in 150 μg mL^{-1} PEO1 solution in 0.1 M KNO_3; (■) first compression of surfaces in solution, following incubation; (●) rapid withdrawal following '■'; (□) compression after replacing PEO1 solution by pure electrolyte, and standing overnight at large D; (○) rapid withdrawal following '□'.

pure electrolyte (open symbols); within error, the profiles are identical. A similar behavior (i.e., similarity of F vs. D profiles before and after replacement of solution) was noted for the case of the lower PEO solution concentration.

Figure 5 shows typical force–distance profiles for *slow compression* (following incubation in 150 μg mL^{-1} PEO1 solution) on a linear–linear scale, corresponding to profiles A in Figures 2 and 4, while the inset to Figure 5 shows the *initial stages* of interaction on an *expanded* linear–linear scale. Figure 6 shows the *final* stages of interaction on a *rapid decompression* of the surfaces, for the same system.

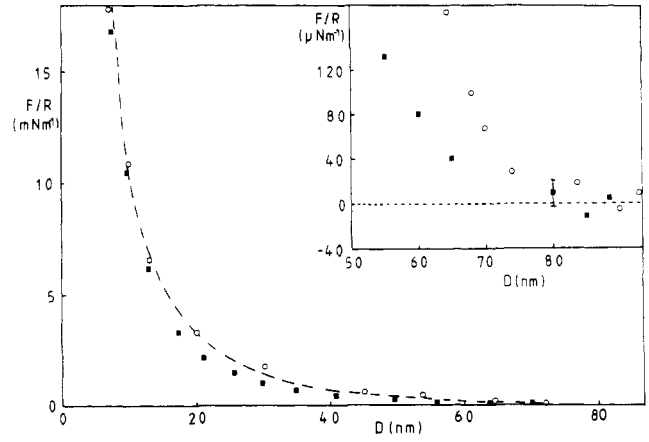

Figure 5. Force–distance profiles between mica surfaces on linear–linear scale following 16 ± 2 h incubation in 150 μg mL^{-1} PEO1 solution in 0.1 M KNO_3: (○) first compression of surfaces, from results of Figure 4; (■) first compression of surfaces, for different experiment (i.e., different pair of mica sheets to those in Figure 4). Inset is as above, on expanded scale. The differences in the (F/R) vs. D profiles (especially near onset of interactions) provide a measure of variation between different experiments. For a given contact position and a given pair of mica sheets the variation is considerably smaller (see, e.g., Figure 2 or Figure 4).

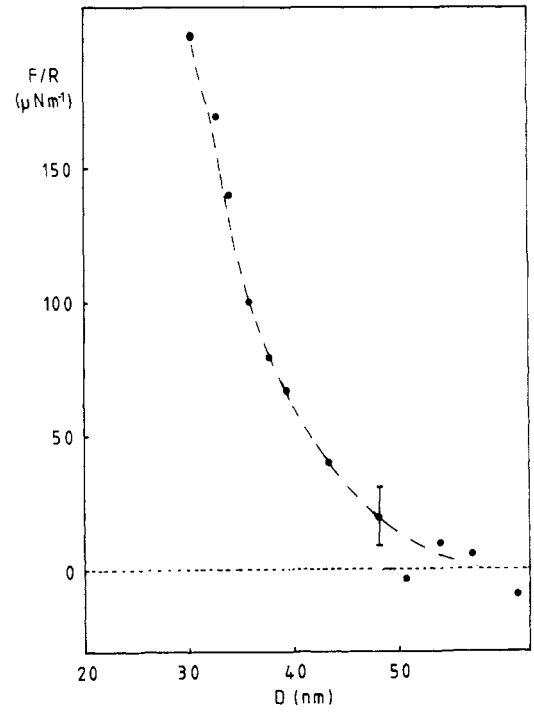

Figure 6. Force–distance profile between mica surfaces following 16 ± 2 h incubation in 150 μg mL^{-1} PEO1 solution in 0.1 M KNO_3, for rapid decompression of the surfaces.

The main feature to note in Figures 5 and 6 is the absence (within error) of any attractive or adhesive component in the interaction.

The refractive index $n(D)$ of the medium between the mica surfaces a distance D apart was determined both before and after incubation on PEO1 solution, and the results are shown in Figure 7. Also shown is $n(D)$ following replacement of PEO solution by pure electrolyte; as for the case of force measurements, (Figure 4) the removal of free polymer from the liquid medium between the surfaces makes little difference (within error) to $n(D)$. Prior to adding polymer the refractive index is essentially independent of D (and close to the value $n = 1.338$ expected for 0.1 mol dm^{-3} KNO_3); following incubation in the polymer solution, $n(D)$ increases down to $D \simeq 5$ nm

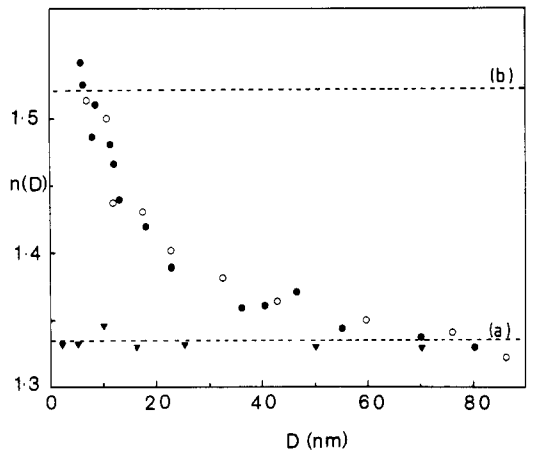

Figure 7. Variation of refractive index $n(D)$ of medium separating mica surfaces a distance D apart: (▼) in 0.1 M KNO_3; (●) following 16 ± 2 h incubation in PEO1 solution (polymer added to 0.1 M KNO_3 to 150 $\mu g\ mL^{-1}$ concentration); (○) after replacement of PEO1 solution by pure electrolyte followed by overnight standing at large D; (broken lines) (a) n (pure 0.1 M KNO_3), (b) n (bulk PEO).

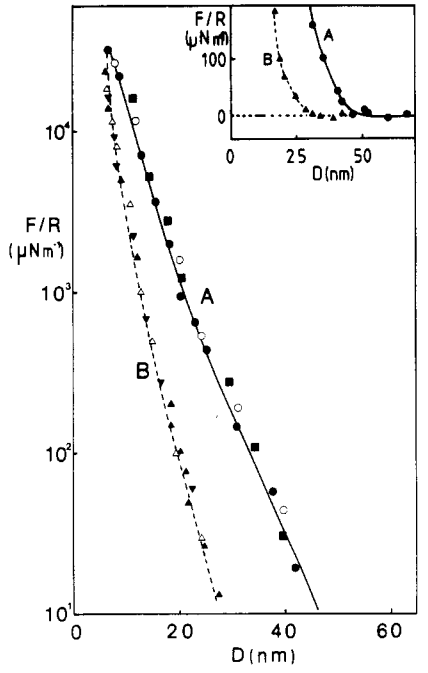

Figure 8. Force–distance profile between curved mica surfaces following 16 ± 2 h incubation in 150 $\mu g\ mL^{-1}$ PEO2 solution in 0.1 M KNO_3: (●) first compression after incubation; (▲) rapid decompression following '●'; (■) immediate rapid recompression following '▲'; (▼) rapid decompression following '■'; (○) compression following replacement of solution by pure electrolyte and overnight standing at large D; (△) rapid decompression following '○'. Inset shows force–distance profile on linear scale. Symbols as above.

(closest approach), where—within error—it attains a value close to that of bulk PEO (n_{PEO} = 1.52).[16] The adsorbance Γ may be estimated from $n(D)$, as previously described;[9] from Figure 5 we find Γ_{PEO1} = 4 ± 1.5 mg m^{-2} of mica surface.

Figures 8, 9, and 10 summarize the force–distance relation and refractive index data following incubation of the mica surfaces in 150 $\mu g\ mL^{-1}$ PEO2 (M = 40 000) solution in 0.1 mol dm^{-3} KNO_3. The basic features are similar to those observed for the case of PEO1 (M = 160 000) presented in Figures 2, 3, and 7, in particular the quasi-equilibrium force profile A (Figure 8) and the "unrelaxed" profile B, corresponding to profiles A and B in Figure 2.

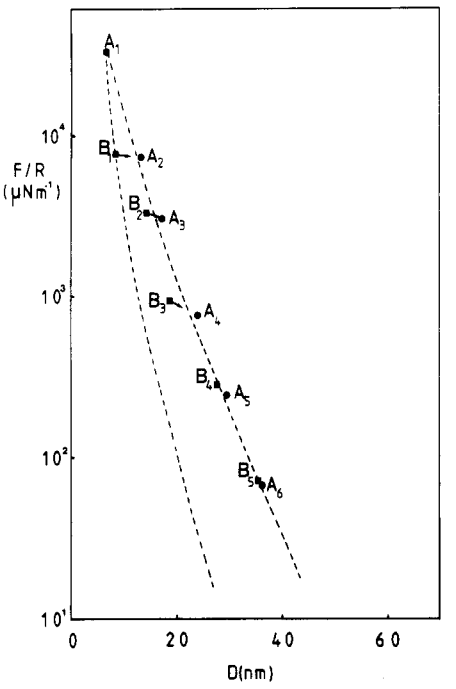

Figure 9. Force–distance profile for same conditions as Figure 8, for slow decompression. Surfaces taken from A_n to B_n, then left for 15 min, whereon they relax spontaneously (→) to the position A_{n+1}, and so on. Further details in text.

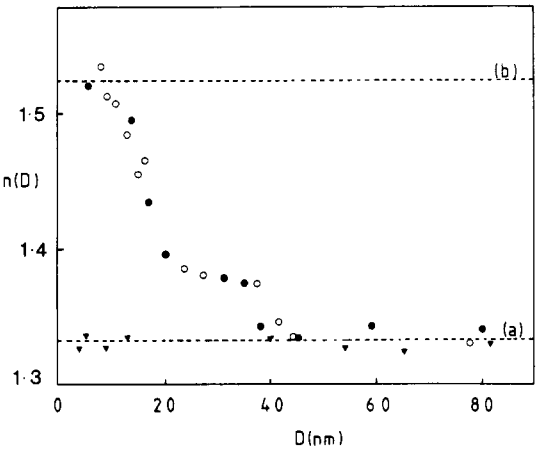

Figure 10. Variation of refractive index $n(D)$ of medium separating mica surfaces a distance D apart: (▼) in 0.1 M KNO_3; (●) following 16 ± 2 h incubation in PEO2 solution (polymer added to 0.1 M KNO_3 to 10 $\mu g\ mL^{-1}$ concentration); (○) after replacement of PEO2 solution by pure electrolyte followed by overnight standing at large D; (broken lines) (a) n (pure 0.1 M KNO_2), (b) n (bulk PEO).

The compression/decompression conditions under which curves A and B (Figure 8) were obtained are those summarized as (i)–(iii) following Figure 2, except that, whereas rapid decompression followed curve B, immediate subsequent recompression always followed *curve A* (in contrast to PEO1, see (iii)). The other main difference is the range at which repulsive interactions are first detected, some 40 nm in contrast to ~75 nm for PEO1. This in turn indicates a lower extension from the surface of the adsorbed layers of the shorter polymer. Replacement of PEO2 solution by pure 0.1 mol dm^{-3} KNO_3 resulted in no significant change in the $F(D)$ profiles (open symbols, Figure 8).

Figure 9 shows $F(D)$ for a slow multistage decompression cycle, as performed for PEO1 (Figure 3). As before the data points fall within the limiting profiles A and B. Finally, Figure 10 shows the variation of $n(D)$ with D before and after incubation in PEO2 solution. The ad-

sorbance indicated from Figure 10 is $\Gamma = 4 \pm 1.5$ mg m^{-2} of mica surface. This value did not sensibly change on replacement of polymer solution by pure electrolyte (open symbols Figure 10).

The results of experiments following incubation in 10 μg mL^{-1} PEO2 solution were closely similar to those in Figures 8, 9, and 10 (at which the polymer concentration was 150 μg mL^{-1}) and are not shown. The main difference between the force profiles obtained following incubation at the lower concentration, relative to those obtained following incubation at the higher concentration (i.e., Figure 8), is that the value of $F(D)$ in the latter case was approximately twice as large, for a given D (as noted for PEO1, see Figures 2 and 4).

Discussion

The exponentially increasing repulsion between the mica surfaces in pure electrolyte prior to addition of polymer (Figure 1) is characteristic of electrostatic double-layer overlap as the surfaces approach and is well described by DLVO theory.[14,15] The Debye length in 0.1 M KNO_3 (from Figure 1) is 1.1 ± 0.1 nm, compared with 1.0 nm for a 1:1 electrolyte of this molarity expected from theory. The mica surface potential ψ_0, evaluated from the $F(D)$ profile via the Gouy–Chapman equation,[14,15] was around 100 mV (several experiments). These results are similar to those reported for the same system by Israelachvili and Adams,[12] who have given a thorough discussion.

Following incubation in polymer solution, *quasi-equilibrium* profiles (A in Figures 2 and 8 and also Figure 5) were indicated for both polymers. Within the error of our force measurements, *no attraction* was detectable as the surfaces approach following overnight adsorption, as indicated in Figures 5 and 6.

Two factors which might lead to an attractive component in the interactions are *depletion layer forces* and polymer *bridging*;[17] the effect of the former, if any, is expected to be beyond our detection capability at the low polymer solution concentrations in the present study, and this is also indicated by the similarity of $F(D)$ both before and after replacement of the PEO solution. If there is any *bridging* attraction in the quasi-equilibrium force law, its contribution must be small relative to the overall repulsion (but see later).

The distance of onset of interactions (for the A profiles, Figures 2 and 8, i.e., ~75 and ~40 nm for PEO1 and PEO2, respectively) is typically twice the extension of the adsorbed polymer layers from the surfaces. In terms of unperturbed radii of gyration R_g (Table I), the extension δ from the surface as detected by our force measurements is thus some $3R_g$ for both polymers. This compares with extensions of some $1.5R_g$ for polystyrene adsorbed onto mica in cyclohexane,[9] under *poor solvent* conditions, and is qualitatively in accord with our expectation that in a moderately *good solvent* system (as for PEO in 0.1 M KNO_3) the adsorbed layers are more extended than for poor or Θ solvents. These extensions compare with the values of δ of some $2–3R_g$ predicted on the basis of mean field theories of adsorbed polymer layers in good solvents,[17,18] and with a (hydrodynamic) layer thickness $\delta \simeq 3R_g$ from a recent light scattering study of PEO (M = 40 000) adsorbed onto polystyrene latex particles in an aqueous medium[19] (a good solvent system). Very recently, ellipsometric measurements[20] on polystyrene adsorbed from good solvents onto a metal surface indicate an ellipsometric thickness of the adsorbed layer $\delta \gtrsim 3R_g$.

The adsorbance Γ of the poly(ethylene oxide) onto the mica surfaces, as estimated from the refractive index profiles (Figures 7 and 10), is some 4 ± 1.5 mg m^{-2} for both PEO1 ($M = 1.6 \times 10^5$) and PEO2 ($M = 4 \times 10^4$). To our knowledge there are no independent measurements of PEO adsorbance onto plane surfaces to compare these values of Γ with. We note, however, that our adsorbance values are higher than for PEO adsorbance onto silica particles (~1 mg m^{-2}). This may be due to a higher affinity of PEO to the mica or possibly because the surface area of the silica particles, determined by N_2 adsorption, was not all accessible to the polymer, for steric reasons.[22] In contrast, for the mica, all the (atomically smooth) surface area is accessible to polymer. Our values of Γ are, however, comparable with those of polystyrene (PS) onto mica in Θ conditions.[23] Our results (Figures 7 and 10) also show (i) that replacement of the solution by pure electrolyte does not lead to desorption and (ii) that compression of the adsorbed layers likewise does not appear to cause polymer to desorb from the surface. This quasi-irreversible adsorption (over the time of our experiments) has implications for the nature of the steric interaction forces between the surfaces (see later). Finally, we note only a weak dependence of the value of Γ on the molecular weight of the polymer (within the experimental error). This contrasts with the case of PS adsorption onto mica in θ conditions[23] but is similar to the case of PS adsorption onto plane surfaces in good solvents, which is also M independent.[20]

The repulsive forces between the mica plates as the adsorbed PEO layers come into overlap are due essentially to osmotic interactions between the opposing segments. We note that water is only a moderately good solvent for PEO, with a polymer–solvent interaction parameter χ = 0.45–0.48;[16,24] the presence of salt in the present system probably reduces the "goodness" of solvent still further. At the very simplest level we might expect that, as the surfaces approach, the mean concentration of polymer in the overlap region will increase, with increasing consequent repulsion. To facilitate further consideration, we present the $F(D)/R$ vs. D data for PEO1 on a double logarithmic plot, Figure 11. This shows a rapid increase in $E(D)$ ($\equiv(1/2\pi)(F(D)/R)$ in the Derjaguin approximation, eq 1) with decreasing D, with a slope $\partial(\log F(D))/\partial(\log D)$ which gradually decreases with decreasing D. At a qualitative level it is not difficult to suggest an explanation for the trend shown in Figure 11, in particular the behavior at the two extremes, (i) when the surfaces just start to interact, $D \lesssim 2\delta \simeq 80$ nm (where δ is the polymer extension from each surface), and (ii) when they are very close together, $D \lesssim 10$ nm. We define $\phi(z)$ as the volume fraction of adsorbed polymer a distance z from the surface and define $\phi_s(\equiv\phi(0))$ as the local volume fraction of polymer *on the mica surfaces* ($\phi_s = 1$ corresponds to occupation by adsorbed polymer of *all* the surface sites). As the opposing adsorbed layers come into overlap, we make the assumption that *nothing else changes*—in particular that ϕ_s does not vary (or alternatively, that ϕ_s varies very slowly relative to the time of our measurements). Then for $D < 2\delta$, the *volume* of overlap per unit area of interacting surface is $v_{overlap} = 2\delta - D$. The mean concentration of polymer in the overlap region is typically exponentially decaying

$$\phi(D/2) \sim \exp(-\alpha D/2) \tag{2}$$

(where α is some inverse correlation length) as has been calculated by a number of approaches.[18] The excess osmotic pressure in the overlap region is then

$$\Pi_{overlap} \sim \nu\phi^2(D/2) \sim e^{-\alpha D} \tag{3}$$

using a mean field expression, where ν is a virial coefficient (though use of scaling exponents would make little dif-

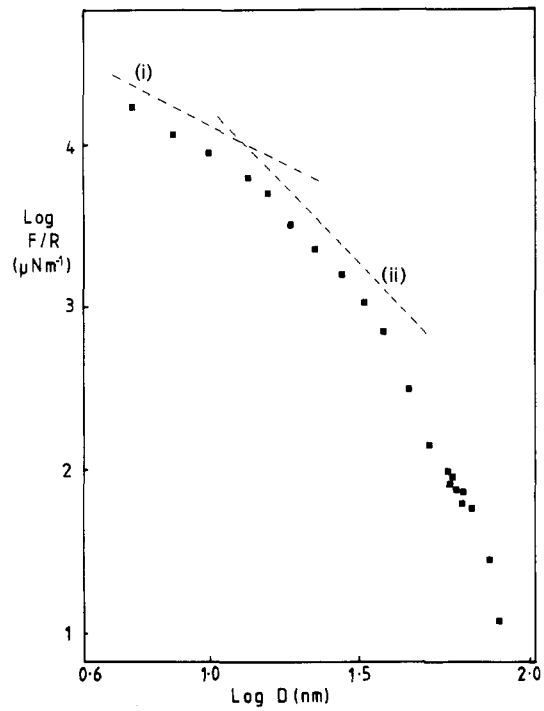

Figure 11. Force–distance profile (on double logarithmic scale) between curved mica surfaces, mean radius R, following incubation in 150 μg mL^{-1} PEO1 solution in 0.1 M KNO_3. Points correspond to solid squares (■) in Figure 5. The broken lines indicate slopes of −1 and −2, corresponding to (i) $E(D) \propto D^{-1}$ and (ii) $E(D) \propto D^{-2}$, respectively, where $E(D) \equiv (F/2\pi R)$ in the Derjaguin approximation. (See also text).

ference to our argument), and the excess interaction energy per unit area varies as

$$E(D) \sim v_{\text{overlap}}\Pi_{\text{overlap}} \sim (2\delta - D)e^{-\alpha D}; \qquad D \lesssim 2\delta \tag{4}$$

Thus, on initial overlap, we have

$$\Delta \equiv \partial(\log E(D))/\partial(\log D) = -D/(2\delta - D) - \alpha D \tag{5}$$

which is very large and negative just at overlap ($D \simeq 2\delta$), while $|\Delta|$ decreases with decreasing D ($D < 2\delta$). This is consistent with the trend indicated on initial overlap in Figure 11.

The other regime, when the surfaces are pressed closely together ($D \lesssim 10$ nm, Figure 11), can also be understood in a relatively straightforward manner. We make the assumptions that the polymer is essentially *uniformly distributed* in the gap at a volume fraction ϕ_{gap} and, as before, that ϕ_s *does not change with* D in this regime (such a condition could for example correspond to $\phi_s \simeq 1$, its limiting value, or else to a ϕ_s changing slowly relatively to the experimental measurements, as previously suggested). Then, since the amount of excess polymer Γ per unit area on the surfaces is fixed, we expect

$$\phi_{\text{gap}} \sim 1/D \tag{6}$$

and the disjoining pressure Π_d (for $\phi_{\text{gap}} \gg \phi_{\text{bulk}}$, the bulk polymer concentration) to be simply the osmotic pressure Π in the gap

$$\Pi_d \simeq \Pi \sim \phi_{\text{gap}}{}^2 \sim D^{-2}$$

(in a mean field approximation). Thus in this regime we expect

$$E(D) \sim D^{-1} \tag{7}$$

For low D values ($\lesssim$10 nm) the variation of $E(D)$ in Figure 11 does appear to tend to a low (inverse) power of D.

In general, however, the assumption of a quasi-fixed ϕ_s used in arguing eq 5 and 7 may not be justified; at the same time the present study appears to be sufficiently direct to merit a closer examination of less-restricted models of steric interaction.[17,18] The crucial point to remember is that the adsorption is irreversible; this implies that *equilibrium* models of steric interactions in which there is exchange with a free polymer solution, which permit *desorption* of polymer on squeezing of the surfaces, may not be appropriate in the present circumstances. (In fact current equilibrium models[17,18] predict *attraction* rather than repulsion, when two surfaces bearing adsorbed polymer layers approach each other, even in good solvents.) A more flexible quantitative framework was recently developed by De Gennes[18] for the case of interactions between adsorbed polymers in Θ and in good solvents and extended by Pincus and one of us[25] to the case of poor solvents. In this approach the interaction energy $E(D)$ between two polymer bearing plates a distance D apart is minimized with respect to the segmental density distribution $\phi(z)$ of polymer away from the wall, and the disjoining pressure $\Pi_d = \partial(E(D))/\partial D$ is then calculated. It is possible to modify this method to the case of fixed adsorbance Γ of polymer on the plates.

The central assumption of the above method (which we may call a generalized Van der Waals approach) is that, subject to a fixed Γ, the values of $\phi(z)$ and in particular ϕ_s are their *equilibrium* values at all surface separations D. A less crucial assumption is that $\phi_s \ll 1$ at all times. For the case of interactions between adsorbed polymers in a *good* solvent, the calculations use a free energy expression with scaling exponents,[18] implying $\phi(z) \ll 1$ at all D (use of a mean field expression for the energy leads to $\Pi_d \to 0$, due to cancellation between attractive surface adsorption and repulsive osmotic contributions). Subject to these, the De Gennes calculation[18] predicts repulsion between the surfaces when overlap between the adsorbed layers occurs, and in detail (i) $E(D) \sim D^{-2}$ for $D \lesssim 2\delta$, i.e., on initial overlap, and (ii) $E(D) \sim D^{-1.25}$ on strongly compressing the surfaces. Reference to Figure 11 shows that on initial overlap $E(D)$ in fact varies considerably more rapidly with D than an inverse square law, though over quite a large range of D(10 nm $\lesssim D \lesssim$ 35 nm) an inverse square relationship is a good fit to the data. Closer in ($D \lesssim$ 10 nm), as already noted, the dependence of $E(D)$ on D is weaker, though in this regime $\phi \gtrsim 0.1$, so that a scaling approach is probably not valid.

The tentative conclusion is that on initial overlap in our experiments the values of $\phi(z)$, especially $\phi(0) \equiv \phi_s$, may not be their equilibrium values, leading to a rapid increase of $E(D)$ with D as argued in eq 5. On further decrease in D, $\phi(z)$ tends toward its equilibrium values and approximate agreement with the De Gennes prediction (the central regime in Figure 11), while on strong compression ϕ_s is again either static or very slowly changing, possibly due to the strong entanglement constraints hindering any rearrangement. In this latter regime ($D \lesssim$ 10 nm) the argument leading to eq 7 is valid; we note that in this range $|\partial(E(D))/\partial D| \simeq 10^6$ N m^{-2}, a value comparable with osmotic pressures of concentrated ($\phi \simeq 0.2$) polymer solutions in moderately good solvents.[16]

The effect on $F(D)$ (or $E(D)$) of rapid separation and recompression of the surfaces (profiles B, Figures 2 and 8) can also be understood in terms of the above discussion. Following compression (e.g., to point C, Figure 2), ϕ_s attains some (high) value. On rapid decompression the value of ϕ_s remains momentarily *higher* than its equilibrium value, with the result that the mean concentration of polymer in the *gap* is *lower* than its equilibrium value, and the disjoining pressure is then lower—i.e., $F(D)$ is apparently smaller, as observed. A rapid partial decompression fol-

lowed by a "waiting time" should take $F(D)$ to its equilibrium value, and this trend is in fact indicated in Figure 3. A more quantitative consideration in terms of the generalized Van der Waals approach (P. Pincus, private communication) leads to a similar conclusion.

Finally, we note that our results contrast with the earlier study by Israelachvili and co-workers,[4] who used a similar method to measure $F(D)$ between mica surfaces in an aqueous solution of a commercial resin consisting mostly of highly polydispersed PEO[26] (Carbowax resin WSR N80, Union Carbide). The main difference is that their results indicated the continuous buildup with time of progressively thicker layers of surface-adsorbed material (up to 1000 nm over 24 h) and also complex short- and long-term hysteretic behavior suggestive of gellike material on the surfaces. This may be due to the polydisperse nature of the polymer as well as the possible presence of microgel or trace chemical impurities in the commercial material used in their experiments.

Acknowledgment. We thank Professor D. Tabor for encouragement and critical reading of the manuscript and Drs. P. Pincus and J. N. Israelachvili for suggestions and comments. We also thank the S.E.R.C. for support of this work.

Registry No. Poly(ethylene oxide) (SRU), 25322-68-3.

References and Notes

(1) Vincent, B. *Adv. Colloid Interface Sci.* **1974**, *4*, 197.
(2) Lyklema, J.; van Vliet, T. *Faraday Discuss. Chem. Soc.* **1978**, *65*, 25.
(3) Cain, F. W.; Ottewill, R. H.; Smitham, J. B. *Faraday Discuss. Chem. Soc.* **1978**, *65*, 33.
(4) Israelachvili, J. N.; Tandon, R. K.; White, L. R. *J. Colloid Interface Sci.* **1980**, *78*, 432.
(5) Doroszkowski, A.; Lambourne, R. *J. Colloid Interface Sci.* **1973**, *43*, 97.
(6) Cairns, R. J. R.; Ottewill, R. H.; Osmond, D. W. J.; Wagstaff, I. *J. Colloid Interface Sci.* **1976**, *54*, 45.
(7) Tabor, D.; Winterton, R. H. S. *Proc. R. Soc. Ser. London A* **1969**, *312*, 435.
(8) Israelachvili, J. N.; Tabor, D. *Proc. R. Soc. London Ser. A* **1972**, *331*, 19.
(9) Klein, J. *J. Chem. Soc., Faraday Trans. 1* **1983**, *79*, 99.
(10) Israelachvili, J. N.; Tirrel, M.; Klein, J.; Almog, Y. *Macromolecules*, submitted for publication. Klein, J.; Luckham, P. F.; Almog, Y. In "Colloidal Particles: Polymer Adsorption and Steric Stabilization"; Goddard, D., Vincent, B., Eds.; American Chemical Society, Washington, DC; in press.
(11) Klein, J.; Luckham, P. F. *Nature (London)* **1982**, *300*, 429.
(12) Israelachvili, J. N.; Adams, G. E. *J. Chem. Soc., Faraday Trans. 1* **1978**, *74*, 975.
(13) Derjaguin, B. V. *Kolloid-Z.* **1934**, *69*, 155.
(14) Derjaguin, B. V.; Landau, L. *Acta Physicochim. URSS* **1941**, *14*, 633.
(15) Verwey, E. J. W.; Overbeek, J. Th. G. "Theory of the Stability of Lyophobic Colloids"; Elsevier: Amsterdam, 1948.
(16) Brandrup, J., Immergut, E. H., Eds. "Polymer Handbook"; Wiley: New York, 1975.
(17) Scheutjens, J. M. H. M.; Fleer, G. J. *Adv. Colloid Interface Sci.* **1982**, *16*, 341, 360.
(18) De Gennes, P.-G. *Macromolecules* **1981**, *14*, 1637; **1982**, *15*, 429.
(19) Cosgrove, T.; Crowley, T. L.; Vincent, B. In "Adsorption from Solution"; Rochester, C., Ottewill, R. H., Eds.; Academic Press: London, 1983.
(20) Kawaguchi, M.; Hayabawa, K.; Tabahashi, A. *Macromolecules* **1983**, *16*, 631.
(21) Rubio, J.; Kitchener, J. A. *J. Colloid Interface Sci.* **1976**, *57*, 132.
(22) McDaniel, M. D.; Hottovy, T. D. *J. Colloid Interface Sci.* **1980**, *78*, 31.
(23) Terashima, H.; Klein, J.; Luckham, P. F. In "Adsorption from Solution"; Rochester, C., Ottewill, R. H., Eds.; Academic Press: London, 1983.
(24) Vincent, B.; Luckham, P. F.; Waite, F. A. *J. Colloid Interface Sci.* **1980**, *73*, 508.
(25) Pincus, P.; Klein, J. *Macromolecules* **1982**, *15*, 1129.
(26) Union Carbide WSR-N80 Product Specification 1-44K N80-1a 70320000, 19-6-1979.

Molecular Aspects of the Rubber Elasticity of Poly(diethylene glycol terephthalate) Networks

Miguel A. Llorente

Departamento de Química General y Macromoléculas, Universidad a Distancia (UNED), Madrid-3, Spain

Evaristo Riande* and Julio Guzmán

Instituto de Plásticos y Caucho (CSIC), Madrid-6, Spain. *Received July 6, 1982*

ABSTRACT: Polymer networks were prepared by end-linking poly(diethylene glycol terephthalate) fractions of number-average molecular weight ranging from 7200 to 11 700 with an aromatic triisocyanate. Stress–strain isotherms carried out on the unswollen networks showed reversibility for elongation ratios α below 5; however, for values of $\alpha > 5$, the isotherms displayed a sharp increase or upturn in the reduced force $[f^*]$, which we attribute to maximum chain extensibility. In general, the networks exhibited a modulus significantly higher than would be expected on theoretical grounds. The theoretical analysis of the experimental results suggests that, for this particular system, there seems to be a high contribution to the elastic modulus from topological entanglements. According to this analysis, the molecular weight between entanglements lies in the vicinity of 2000. In order to get confirmatory evidence on the presence of entanglements in the fractions used in the preparation of the networks, dynamic viscoelastic measurements were carried out on un-cross-linked fractions lying in the range 4600–24 700. The time–temperature superposition principle was applied to the dynamic moduli to establish forms for the plateau and terminal responses, from which the relaxation spectra corresponding to these regions were determined. The presence of a minimum in the spectra separating the two sets of relaxation times corresponding to motions within entanglements and motions across entanglements loci suggests that relatively well-developed entanglements are already present in the low molecular weight fractions used in the preparation of the networks.

Introduction

A controversial and important issue in the investigation of rubber elasticity that needs to be clarified is whether or not the topological entanglements contribute to the equilibrium elastic properties of amorphous polymer networks. In this regard, whereas some authors find a big

0024-9297/84/2217-1048$01.50/0